Reactions of Laser-Ablated Beryllium Atoms with Hydrogen Cyanide in Excess Argon. FTIR Spectra and Quantum Chemical Calculations on BeCN, BeNC, HBeCN, and HBeNC

Dominick V. Lanzisera and Lester Andrews*

Contribution from the Department of Chemistry, University of Virginia, Charlottesville, Virginia 22901

Received March 7, 1997[⊗]

Abstract: Laser-ablated beryllium atoms have been reacted with hydrogen cyanide ($H^{12}CN$, $H^{13}CN$, and $D^{12}CN$) during condensation in excess argon at 6−7 K. In the matrix infrared spectrum, the major products observed are BeNC, BeCN, HBeNC, and HBeCN. Consistent with typical beryllium bonding, these new beryllium species are linear molecules. Density functional theory calculations on these products with the BP86 functional and 6-311G* basis sets predict vibrational frequencies extremely well, even for HBeCN where mixing between the nearly isoenergetic Be−H and C≡N stretching modes causes significant complications in the spectra. Although B3LYP and MP2 calculations are more sophisticated than the BP86 method, they do not predict the vibrational frequencies of these products nearly as well. More important is the carbon 12/13 isotopic frequency ratio as a description of the normal modes, and the BP86 method generates 12/13 ratios much closer to observed values for HBeCN than frequency ratios from the more time-consuming CISD method.

Introduction

In studies of alkali cyanides, the potential energy surface was computed to be flat in the coordinate describing the metal position around the CN.[1−5] The bonding between the metal and cyanide was almost entirely ionic, and the ground state structure for these molecules was described as T-shaped, not linear. By contrast, Bauschlicher et al. calculated alkaline earth cyanides and found that all such molecules prefer the linear isocyanide structure.[6] A barrier to interconversion to the linear cyanide structure exists for the smaller molecules, BeNC and MgNC, but not for CaNC and BaNC. Although this barrier is only 0.23 eV at the SCF-CI level for MgNC, the barrier is much more substantial for BeNC at 0.71 eV. These calculations suggest that beryllium cyanides exist in a linear form as either the cyanide or isocyanide with no stable intermediate structure.

The first laser ablation matrix infrared experiments with beryllium uncovered several new compounds. Reactions of Be with H_2, O_2, and H_2O generated molecules such as BeH_2, ArBeO, OBeO, and HBeOH.[7−11] For each of these products, the geometry about Be was linear with sp hybridization, the preferred geometry for alkaline earth species.

In a matrix isolation study of the reactions of laser-ablated Be with C_2H_2, the major new products were determined to be the linear species BeCCH and HBeCCH.[12] Because acetylene is isoelectronic with hydrogen cyanide, these products can be viewed as analogues of BeCN and HBeCN, respectively. This study substitutes HCN for C_2H_2 in an attempt to observe and characterize beryllium cyanides with and without hydrogen and to determine their structures. The BeCCH and HBeCCH molecules were characterized by DFT/B3LYP[13−15] frequency calculations to support the vibrational assignments. Here, we will compare the pure DFT functional, BP86,[16,17] with the hybrid B3LYP functional as well as the MP2[18−20] and CISD[21−23] methods, to help identify these new molecules.

A previous study of reactions of laser-ablated boron with hydrogen cyanide produced the linear products BNC and BCN, as well as the nonlinear products HBNC and HBCN.[24] Also present in the product spectra was the cyclic molecule HB(CN), where the boron is bonded to both the carbon and nitrogen. Because Be orbitals do not usually adopt sp^2 or sp^3 hybridization, all products, in contrast to B compounds, should be linear. The results presented in this article demonstrate that four new beryllium cyanide products are formed and trapped in solid argon, and all of these products have linear geometries.

[⊗] Abstract published in *Advance ACS Abstracts,* June 15, 1997.

(1) Törring, T.; Bekooy, J. P.; Meerts, W. L.; Hoeft, J.; Tiemann, E.; Dymanus, A. *J. Chem. Phys.* **1980**, *73*, 4875.
(2) van Vaals, J. J.; Meerts, W. L.; Dymanus, A. *Chem. Phys.* **1984**, *86*, 147.
(3) Wormer, P. E. S.; Tennyson, J. *J. Chem. Phys.* **1981**, *75*, 1245.
(4) Klein, M. L.; Goddard, J. D.; Bounds, D. G. *J. Chem. Phys.* **1981**, *75*, 3909.
(5) Marsden, C. J. *J. Chem. Phys.* **1982**, *76*, 6451.
(6) Bauschlicher, C. W., Jr.; Langhoff, S. R.; Partridge, H. *Chem. Phys. Lett.* **1985**, *115*, 124.
(7) Tague, T. J., Jr.; Andrews, L. *J. Am. Chem. Soc.* **1993**, *115*, 12111.
(8) Thompson, C. A.; Andrews, L. *J. Am. Chem. Soc.* **1994**, *116*, 423.
(9) Thompson, C. A.; Andrews, L. *J. Chem. Phys.* **1994**, *100*, 8689.
(10) Andrews, L.; Chertihin, G. V.; Thompson, C. A.; Dillon, J.; Byrne, S.; Bauschlicher, C. W., Jr. *J. Phys. Chem.* **1996**, *100*, 10088.
(11) Thompson, C. A.; Andrews, L. *J. Phys. Chem.* **1996**, *100*, 12214.
(12) Thompson, C. A.; Andrews, L. *J. Am. Chem. Soc.* **1996**, *118*, 10242.
(13) Lee, C.; Yang, W.; Parr, R. G. *Phys. Rev. B* **1988**, *37*, 785.
(14) Miehlich, B.; Savin, A.; Stoll, H.; Preuss, H. *Chem. Phys. Lett.* **1989**, *157*, 200.
(15) Becke, A. D. *J. Chem. Phys.* **1993**, *98*, 5648.
(16) Becke, A. D. *Phys. Rev. A* **1988**, *38*, 3098.
(17) Perdew, J. P. *Phys. Rev. B* **1986**, *33*, 8822.
(18) Head-Gordon, M.; Pople, J. A.; Frisch, M. J. *Chem. Phys. Lett.* **1988**, *153*, 503.
(19) Frisch, M. J.; Head-Gordon, M.; Pople, J. A. *Chem. Phys. Lett.* **1990**, *166*, 275.
(20) Frisch, M. J.; Head-Gordon, M.; Pople, J. A. *Chem. Phys. Lett.* **1990**, *166*, 281.
(21) Pople, J. A.; Seeger, R.; Krishnan, R. *Int J. Quantum Chem. Symp.* **1977**, *11*, 149.
(22) Krishnan, R.; Schlegel, H. B.; Pople, J. A. *J. Chem. Phys.* **1980**, *72*, 4654.
(23) Raghavachari, K.; Pople, J. A. *Int J. Quantum Chem.* **1981**, *20*, 167.
(24) Lanzisera, D. V.; Andrews, L.; Taylor, P. R. *J. Phys. Chem. A* In press.

S0002-7863(97)00740-3 CCC: $14.00

Experimental Section

The apparatus for pulsed laser ablation, matrix isolation, and FTIR spectroscopy has been described previously.[24−26] Mixtures of 0.3% HCN, H^{13}CN or DCN in Ar codeposited at 3 mmol/h for 2 h onto a 6−7 K cesium iodide window react with beryllium atoms ablated from a target source (Johnson-Matthey, lump, 99.5% Be) rotating at 1 rpm. The fundamental 1064-nm beam of a Nd:YAG laser (Spectra Physics DCR-11) operating at 10 Hz and focused with a $f = +10$ cm lens ablated the target using 20−30 mJ per 10 ns pulse. The procedure for preparing HCN was described previously.[24,27] For DCN, we added D_2SO_4 (Aldrich) and D_2O (Aldrich) to solid KCN (Aldrich) and, because of prior HCN passivation of the manifold, the H/D ratio approached unity. For H^{13}CN, we added concentrated HCl to K^{13}CN (Cambridge Isotopes) and obtained a ^{13}C enrichment of greater than 80%. Following deposition, a Nicolet 550 Fourier transform infrared (FTIR) spectrometer collected infrared spectra from 4000 to 400 cm^{-1} by using a liquid nitrogen cooled MCT detector; the resolution was 0.5 cm^{-1} with a frequency accuracy of ± 0.2 cm^{-1}. After sample deposition, annealing to 15 K followed by broadband (240−580 nm) mercury arc photolysis (Philips 175 W) produced changes in the FTIR spectra. Further annealings to 25 and 35 K also changed some of the spectral features.

We perfomed density functional theory (DFT) and Hartree−Fock (HF) calculations on potential product molecules using the Gaussian 94 program package.[28] Calculations used either the BP86 pure DFT functional, the B3LYP hybrid DFT functional, the MP2 method, or configuration interaction with singles and doubles (CISD). All calculations employed the 6-311G* basis sets for each atom[29,30] or for comparison in BP86 calculations, Dunning's correlation consistent double ζ-basis set (cc-pVDZ)[31,32] for the H, C, and N atoms, plus the D95* basis sets for Be atoms.[33] The geometry optimizations used redundant internal coordinates and converged via the Berny optimization algorithm,[28,34] and the program calculated vibrational frequencies analytically. Of the four methods, the least expensive BP86/6-311G* calculations provided the best results, as will be described.

Results

Matrix infrared spectra for various isotopic combinations are reported as well as the relative change in intensity of product peaks following broadband photolysis and subsequent annealing to 25 K. Besides the beryllium product peaks mentioned in this section, we observed bands for HNC and CN, apparently formed from radiation in the ablation process.[35] Also, oxides such as the $(BeO)_2$ ring at 866.3 and 1131.2 cm^{-1}, BeOBe at 1412.4 cm^{-1}, and Ar−BeO at 1526.1 cm^{-1} are formed[8−10] due to oxides on the target surface and reaction of beryllium with residual H_2O or D_2O from the synthesis of HCN or DCN.

Be + H^{12}CN. Table 1 lists all the observed frequencies as well as the photolysis and 25 K annealing behavior for all frequencies. Figure 1a presents the best spectrum in the 2220−1960-cm^{-1} range for reactions of Be with H^{12}CN with use of an ablation energy near 30 mJ. This frequency range represents the majority of the Be−H and C≡N stretching regions, and the presence of BeH, BeH_2, and CN indicates that both Be−H and C≡N vibrational modes of products may be present in this spectrum.[7,32] The strongest absorption, labeled A, at 2088.7 cm^{-1} decreases by nearly half on photolysis. A band to the red of this absorption, labeled C, increases a small amount on photolysis and declines by a smaller amount on annealing; the peak at 2153.2 cm^{-1}, also labeled C, exhibits similar photolysis and annealing behavior. Near the high-energy end of the spectrum, a band labeled D increases 35% on photolysis and decreases by a similar percentage on annealing. A weak band also labeled D tracks with the 2202.8-cm^{-1} peak on photolysis and annealing and suggests the possibility that these bands represent different vibrational modes of the same product. Another weak absorption labeled B at 2183.1 cm^{-1} broadens and increases enormously on photolysis, then sharpens with a moderate decrease in total intensity on 25 K annealing.

The Be−C and Be−N regions of the spectrum from 950 to 740 cm^{-1} are presented in Figure 2a. The largest absorptions occur in the higher energy region of this spectrum and are labeled A and C. The A band declines 45% on photolysis, while the 912.4-cm^{-1} peak increases a small amount. A weaker band at 805.8 cm^{-1} increases tremendously on photolysis then sharpens on annealing, thereby indicating that this band, labeled

Table 1. Observed Frequencies (cm^{-1}) of Products from Beryllium−Hydrogen Cyanide Reactions

12/1[a]	13/1[a]	12/2[a]	phot/ann[b]	identity
2202.8	2165.6	2194.2	+35/−35	HBeCN
2183.1	2134.6	2183.1	+620/−60	BeCN
2159.4	2159.4	1674.2	+5/−5	BeH_2
2153.2	2149.5	1631.3	+20/−10	HBeNC
2128.6	2116.7	1642.1	+35/−35	HBeCN
2088.7	2050.8	2088.7	−45/−5	BeNC
2085.7	2050.9	2098.6	+20/−10	HBeNC
2044.3	2002.0	2044.3	−10/−60	CN
1971.0	1971.0	1477.3	+10/+10	BeH
938.4	932.0	938.4	−45/−5	BeNC
912.4	906.0	895.6	+20/−10	HBeNC
805.8	802.2	805.8	+620/−60	BeCN
800.1	795.3	750.9	+35/−35	HBeCN
530.1	528.3	436.1	+35/−35	HBeCN
		431.5	+35/−35	HBeCN
525.4	545.4	422.1	+20/−10	HBeNC
521.7	521.7	418.0	+20/−10	HBeNC

[a] Isotopes for carbon/hydrogen. [b] Percent increase or decrease on photolysis/annealing to 25 K.

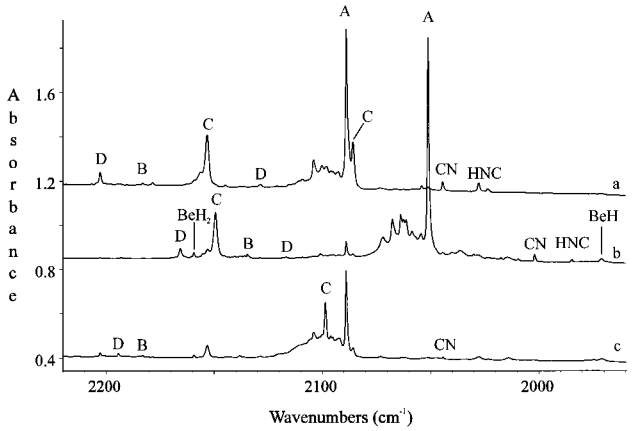

Figure 1. Matrix infrared spectra in the 2220−1960-cm^{-1} Be−H and C≡N stretching regions following pulsed laser ablation of Be atoms codeposited with Ar/HCN (300/1) samples on a CsI window at 6−7 K: (a) Be + H^{12}CN, (b) Be + H^{13}CN, and (c) Be + D^{12}CN.

(25) Lanzisera, D. V.; Andrews, L. *J. Phys. Chem. A* **1997**, *101*, 824.
(26) Lanzisera, D. V.; Andrews, L. *J. Phys. Chem. A* **1997**, *101*, 1482.
(27) Bohn, R. B.; Andrews, L. *J. Phys. Chem.* **1989**, *93*, 3974.
(28) Gaussian 94, Revision B.1: Frisch, M. J.; Trucks, G. W.; Schlegel, H. B.; Gill, P. M. W.; Johnson, B. G.; Robb, M. A.; Cheeseman, J. R.; Keith, T.; Petersson, G. A.; Montgomery, J. A.; Raghavachari, K.; Al-Laham, M. A.; Zakrzewski, V. G.; Ortiz, J. V.; Foresman, J. B.; Cioslowski, J.; Stefanov, B. B.; Nanayakkara, A.; Challacombe, M.; Peng, C. Y.; Ayala, P. Y.; Chen, W.; Wong, M. W.; Andres, J. L.; Replogle, E. S.; Gomperts, R.; Martin, R. L.; Fox, D. J.; Binkley, J. S.; Defrees, D. J.; Baker, J.; Stewart, J. P.; Head-Gordon, M.; Gonzalez, C.; Pople, J. A.; Gaussian, Inc.: Pittsburgh, PA, 1995.
(29) McLean, A. D.; Chandler, G. S. *J. Chem. Phys.* **1980**, *72*, 5639.
(30) Krishnan, R.; Binkley, J. S.; Seeger, R.; Pople, J. A. *J. Chem. Phys.* **1980**, *72*, 650.
(31) Kendall, R. A.; Dunning, T. H., Jr.; Harrison, R. J. *J. Chem. Phys.* **1992**, *96*, 6796.
(32) Dunning, T. H., Jr. *J. Chem. Phys.* **1989**, *90*, 1007.
(33) Dunning, T. H., Jr.; Hay, P. J. In *Modern Theoretical Chemistry*; Schaefer, H. G., III, Ed.; Plenum: New York, 1976; pp 1−28.
(34) Schlegel, H. B. *J. Comput. Chem.* **1982**, *3*, 214.
(35) Milligan, D. E.; Jacox, M. E. *J. Chem. Phys.* **1967**, *47*, 278.

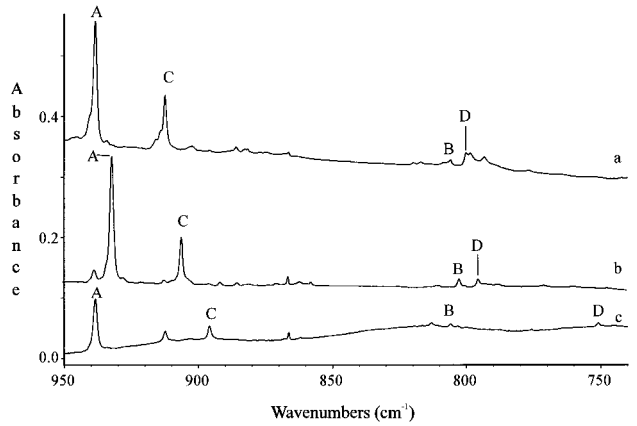

Figure 2. Matrix infrared spectra in the 950−740-cm^{-1} Be−N and Be−C stretching regions following pulsed laser ablation of Be atoms codeposited with Ar/HCN (300/1) samples on a CsI window at 6−7 K: (a) Be + H^{12}CN, (b) Be + H^{13}CN, and (c) Be + D^{12}CN.

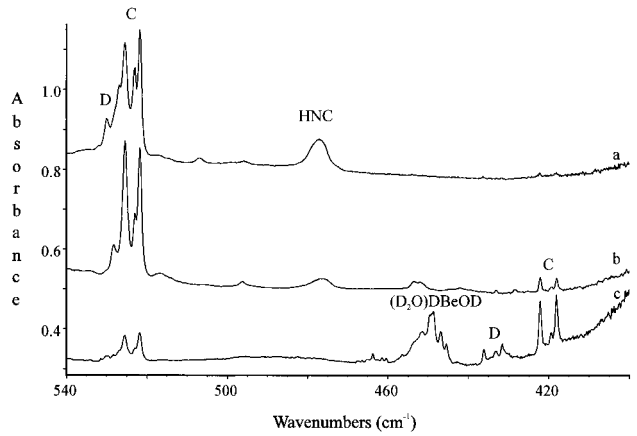

Figure 3. Matrix infrared spectra in the 540−400-cm^{-1} bending region following pulsed laser ablation of Be atoms codeposited with Ar/HCN (300/1) samples on a CsI window at 6−7 K: (a) Be + H^{12}CN, (b) Be + H^{13}CN, and (c) Be + D^{12}CN. The cluster near 450 cm^{-1} is due to DBeOD complexed with D_2O from the exchange reaction (see ref 11).

B, tracks with the band labeled B in Figure 1a. The HCN cluster peak near 800 cm^{-1} contains a weak product band at 800.1 cm^{-1}, labeled D, which increases about a third on photolysis and decreases about a third on 25 K annealing.

In the bending region (Figure 3a), the linear bend of HNC at 477.1 cm^{-1} can be observed, but the spectrum is dominated by a cluster of peaks near 525 cm^{-1}. These absorptions, at 530.1, 526.9, 525.4, 523.2, and 521.7 cm^{-1}, all increase modestly upon broadband photolysis and decrease on 25 K annealing.

Be + H^{13}CN. Figure 1b presents the spectrum for the Be−H and C≡N stretching regions for products of the reaction of Be with isotopically enriched H^{13}CN. The largest absorption, labeled A, decreases about 35% on photolysis and tracks reasonably well with the A band in Figure 1a. Because of the residual H^{12}CN in this experiment, a trace of the 2088.7-cm^{-1} band remained. Notable is that there is no red shoulder to the large band in Figure 1b as there was in Figure 1a. The next largest absorption, labeled C, tracks with the 2153.2- and 2085.7-cm^{-1} bands from the Be + H^{12}CN experiment, and the small isotopic carbon shift from the 2153.2-cm^{-1} peak suggests a Be−H stretch. A weaker absorption at 2165.6 cm^{-1}, labeled D, tracks with the peaks labeled D in Figure 1a. Among the weaker bands, a peak at 2134.6 cm^{-1} exhibits the same large intensity increase upon photolysis as the ^{12}C counterpart at 2183.1 cm^{-1}, while a faint peak at 2116.7 cm^{-1} tracks with the other absorptions labeled D.

In Figure 2b, identifying ^{12}C/^{13}C partners is fairly straighforward. Both the A band and C band exhibit a 6.4 cm^{-1} isotopic carbon shift with respect to their natural isotopic counterparts, while the lack of a HCN cluster band near 800 cm^{-1} makes for clearer observation of the product peaks in this region of the spectrum. The B and D peaks shift 3.6 and 4.8 cm^{-1}, respectively, upon carbon-13 substitution.

In the bending region (Figure 3b), the large cluster of peaks is, with one exception, unshifted given the resolution of the instrument. However, the blue shoulder at 530.1 cm^{-1} in Figure 3a shifts to 528.3 cm^{-1} in Figure 3b, indicating that this cluster of peaks is due to at least two product molecules.

Be + DCN. Figure 1c presents the best Be + DCN product spectrum for the C≡N stretching region. Some of the peaks are about half as large as in the HCN experiments, while others are even weaker. Because beryllium can also react with the D_2O in the sample, the yield of products from the DCN reaction was reduced.[11] Bands in Figure 1c that are about half the intensity of those in Figure 1a belong to products without hydrogen. The weaker bands are those of residual products with hydrogen. For example, the strong absorption at 2088.7 cm^{-1} belongs to a product without hydrogen, but the C band at 2153.2 cm^{-1} corresponds to a molecule with hydrogen. The strongest new peak, at 2098.6 cm^{-1}, appears to track with the C peaks of Figure 1, parts a and b. At the high-energy end of the spectrum, an absorption labeled D tracks with the 2202.8-cm^{-1} band from Figure 1a and is about the same size as this band in the DCN experiment.

In the Be−D stretching region, two new absorptions accompany BeD_2 at 1674.2 cm^{-1}. The first peak, at 1631.3 cm^{-1}, tracks with the upper C bands. The other peak, at 1642.1 cm^{-1}, increases more on photolysis and decreases more on annealing, thereby tracking with the D bands of Figure 1, parts a and b.

In Figure 2c, the intensity of the 938.4-cm^{-1} absorption indicates that this peak, like the other bands labeled A, possesses no hydrogen atoms. By contrast, the C band at 912.4 cm^{-1} is much smaller in this figure and has a tracking deuterated counterpart at 895.6 cm^{-1}. A similar contrast occurs near 800 cm^{-1}, where the 805.8-cm^{-1} band does not shift, but the 800.1-cm^{-1} band shifts to 750.9 cm^{-1}.

In Figure 3c, the cluster of peaks highlighted by a doublet at 525.4 and 521.7 cm^{-1} is much weaker, and two new clusters appear, indicating that the original cluster consisted of two sets of product bands which have different hydrogen isotopic shifts. The largest of these new doublets, at 422.1 and 418.0 cm^{-1}, increases 20% on photolysis and decreases 10% on annealing, while the doublet at 436.1 and 431.5 cm^{-1} increases 35% on photolysis and is reduced by a similar amount on annealing. The cluster of peaks near 450 cm^{-1} is due to DBeOD complexed with D_2O from the exchange reaction.[11]

Calculations. Table 2 lists the results for BP86 calculations for four possible product molecules in the Be + HCN reaction. Because beryllium is an alkaline earth element, only those products with linear geometries are included. The spectra give no evidence of products with two cyanide groups, so these calculations were not performed.

Frequencies calculated by different methods for comparison with experiment are presented in Table 3. Calculated frequencies for BeCN and BeNC show that the BP86 approach generally predicts lower vibrational energies than B3LYP calculations. The MP2 level is better than the B3LYP approach and only slightly worse than the BP86 method for BeNC, but yields unreasonable frequencies for BeCN. With the BP86 method, use of the more inclusive basis sets, cc-pVDZ with D95*, tends to generate slightly higher vibrational frequencies

Table 2. DFT/BP86 Calculations for Products of Reactions of Be with HCN

species	energy (au)	bond lengths (Å)[a]	freq in cm^{-1} (int in km mol^{-1})[b]
HBeNC	−108.20564	$r_{HBe} = 1.33$; $r_{BeN} = 1.53$; $r_{CN} = 1.19$	2179.2 (305), 2066.9 (217), 918.9 (90), 565.0 (214 × 2), 172.1 (4 × 2)
HBeCN	−108.20091	$r_{HBe} = 1.33$; $r_{BeC} = 1.66$; $r_{CN} = 1.17$	2223.1 (167), 2147.4 (61), 799.5 (77), 554.7 (203 × 2), 232.5 (13 × 2)
BeNC	−107.55429	$r_{BeN} = 1.54$; $r_{CN} = 1.19$	2067.1 (368), 938.2 (129), 173.1 (0 × 2)
BeCN	−107.54833	$r_{BeC} = 1.67$; $r_{CN} = 1.17$	2199.3 (83), 806.6 (114), 243.6 (4 × 2)

[a] All products are linear molecules. [b] For the major stable isotope.

Table 3. DFT Calculations of Vibrational Frequencies and Intensities for BeCN and BeNC with Different Combinations of Functionals and Basis Sets

	method/basis set			
	BP86/6-311G*	BP86/cc-pVDz[a]	B3LYP/6-311G*	MP2/6-311G*
BeCN				
C≡N stretch[b]	2199.3 (83) ↔ 2149.5 (76)	2208.4 (85) ↔ 2158.1 (77)	2291.0 (72) ↔ 2239.3 (65)	4090.4 (2036) ↔ 3999.9 (1966)
$^{12}C/^{13}C$ ratio[c]	1.02317	1.02331	1.02309	1.02263
Be−C stretch[b]	806.6 (114) ↔ 804.1 (114)	833.4 (132) ↔ 831.0 (132)	827.7 (120) ↔ 825.1 (120)	832.4 (134) ↔ 829.4 (132)
$^{12}C/^{13}C$ ratio[c]	1.00311	1.00289	1.00315	1.00362
Be−C−N bend[b]	243.6 (2 × 4) ↔ 237.4 (2 × 4)	261.4 (2 × 2) ↔ 254.7 (2 × 2)	260.7 (2 × 4) ↔ 254.0 (2 × 3)	258.4 (2 × 6) ↔ 251.7 (2 × 5)
$^{12}C/^{13}C$ ratio[c]	1.02612	1.02631	1.02638	1.02662
BeNC				
C≡N stretch[b]	2067.1 (368) ↔ 2029.0 (367)	2083.1 (317) ↔ 2045.1 (318)	2146.0 (396) ↔ 2106.3 (395)	2083.6 (283) ↔ 2045.5 (285)
$^{12}C/^{13}C$ ratio[c]	1.01878	1.01858	1.01885	1.01863
Be−N stretch[b]	938.2 (129) ↔ 931.2 (124)	944.0 (147) ↔ 936.9 (142)	969.6 (139) ↔ 962.5 (134)	947.0 (155) ↔ 939.8 (150)
$^{12}C/^{13}C$ ratio[c]	1.00752	1.00758	1.00738	1.00873
Be−N−C bend[b]	173.1 (2 × 0) ↔ 171.7 (2 × 0)	152.4 (2 × 1) ↔ 151.1 (2 × 1)	186.8 (2 × 0) ↔ 185.3 (2 × 0)	167.0 (2 × 0) ↔ 165.5 (2 × 0)
$^{12}C/^{13}C$ ratio[c]	1.00815	1.0086	1.00863	1.00906

[a] cc-pVDZ basis set on C and N atoms and D95* basis set on Be. [b] Vibrational frequencies in cm^{-1} and intensities in km mol^{-1} in parentheses for ^{12}C ↔ ^{13}C isotopes. [c] Ratio of ^{12}C isotope frequency to ^{13}C isotope frequency.

than with the 6-311G* basis sets. The ratios of the carbon-12 and carbon-13 isotopic frequencies, as a characteristic of the normal modes, are effectively independent of the method used for these molecules.

Discussion

Four products have been identified in these experiments by using isotopic data and BP86 calculations. Unlike with reactions of B with HCN, no cyclic compounds with a Be(CN) ring structure are observed, and this results from Be preferring linear geometries and a coordination number of no more than 2.

Species A: BeNC. The strong absorptions at 2088.7 cm^{-1} in Figure 1, parts a and c, and 2050.8 cm^{-1} in Figure 1b correspond to the C≡N stretching motion of beryllium isocyanide, BeNC. The BP86 calculations predict this product to be 3.7 kcal mol^{-1} more stable than BeCN, while no stable cyclic Be(CN) compound would converge. Table 3 lists the observed frequencies for BeNC, as well as the results of these calculations. The strong absorptions at 938.4 and 932.0 cm^{-1}, for $BeN^{12}C$ and $BeN^{13}C$, respectively, are nearly identical with the predicted values, while calculations of the C≡N stretching frequencies are still only about 1% lower than the observed values. The calculated intensities for both these vibrational absorptions (Table 2) are more than 100 km mol^{-1}, with the C≡N stretch nearly three times more intense than the Be−N stretch. For both peaks, the intensities for the DCN experiments are competitive with those for the HCN experiments, suggesting an absence of hydrogen in the molecule.

Compared to boron isocyanide,[24] beryllium isocyanide has a C≡N stretch about 20−30 cm^{-1} higher in energy. This value is much lower than the 2171-cm^{-1} value for BCN and confirms the assignment of these strong bands to BeNC. Also, the B−N stretch in BNC lies higher than the B−C stretch of BCN, and the presence of strong bands at 938.4 and 932.0 cm^{-1} in the high-energy region of Figure 2 suggests that these absorptions correspond to Be−N stretching vibrations.

Species B: BeCN. Although BeCN is calculated to be of nearly the same energy as BeNC, no other strong absorption in the C≡N stretching region retains a large fraction of its intensity in the DCN experiments. According to Table 2, the Be−C stretch should be the strongest absorption for this molecule and occur near 800 cm^{-1}. The absorptions observed at 805.8 and 802.2 cm^{-1} are also strong in the DCN experiments and are nearly identical with the predicted values. Table 4 also presents observed and calculated frequencies for BeCN. The photolysis and annealing behavior of these absorptions are unique in this experiment and are an identifying characteristic of BeCN peaks. The C≡N stretching modes that mimic this behavior are at 2183.1 and 2134.6 cm^{-1} for $Be^{12}CN$ and $Be^{13}CN$, respectively. As with the Be−C stretching mode, these computationally inexpensive DFT calculations predict vibrational frequencies within 1% of their experimental values. These absorptions are not among the most intense in Figure 1, but the BP86 calculations predict them to be less than one quarter as intense as the BeNC bands given equal concentrations of both products.

Table 4. Observed and BP86/6-311G* Calculated Vibrational Frequencies (cm^{-1}) for BeCN and BeNC

	$Be^{12}CN$	$Be^{13}CN$	$BeN^{12}C$	$BeN^{13}C$
obsd	2183.1	2134.6	2088.7	2050.8
calcd	2199.3	2149.5	2067.1	2029.0
scale factor[a]	1.007	1.007	0.990	0.989
obsd	805.8	802.2	938.4	932.0
calcd	806.6	804.1	938.2	931.2
scale factor[a]	1.001	1.002	1.000	0.999
calcd	243.6	237.4	173.1	171.7

[a] Calculated frequency divided by observed frequency.

On the basis of a comparison with BCN and BNC, one expects the C≡N stretching frequency of BeCN to be about 100 cm^{-1} higher in energy, and that is the case in these experiments. For the isoelectronic BeCCH molecule,[12] the Be−C stretching motion absorbs at 855.0 cm^{-1} when both carbons are ^{12}C. This frequency changes to 851.8 cm^{-1} when the first (i.e., bonded to Be) carbon is changed to ^{13}C. The small carbon isotopic shift in BeCCH and BeCN, especially relative to BeNC, suggests a mode that behaves like a "sym-

Table 5. Experimental, BP86/6-311G*, and CI/6-311G* Vibrational Frequencies (cm^{-1}) for HBeCN and HBeNC

	$HBe^{12}CN$	$HBe^{13}CN$	$DBe^{12}CN$	$HBeN^{12}C$	$HBeN^{13}C$	$DBeN^{12}C$
obsd	2202.8	2165.6	2194.2	2153.2	2149.5	1631.3
calcd-BP86	2223.1	2187.5	2212.5	2179.2	2177.7	1646.4
calcd-CI	2350.4	2301.2	2345.6	2258.7	2253.8	1702.9
obsd	2128.6	2116.8	1642.1	2085.7	2050.9	2098.6
calcd-BP86	2147.4	2132.7	1627.8	2066.9	2030.3	2078.4
calcd-CI	2223.9	2220.0	1680.5	2190.5	2154.3	2207.6
obsd	800.1	795.3	750.9	912.4	906.0	895.6
calcd-BP86	799.5	796.8	760.0	918.9	911.7	867.4
calcd-CI	820.9	818.0	780.8	953.1	945.9	899.6
obsd	530.1	528.3	436.1/431.5	525.4/521.7	525.4/521.7	422.1/418.0
calcd-BP86	554.7	552.7	464.8	565.0	565.0	464.1
calcd-CI	579.7	577.5	485.8	599.1	599.0	491.3

metric" stretching mode with little carbon motion. A similar situation exists when comparing BCN and BNC.[24]

Species C: HBeNC. The strongest band with HCN (Figure 1a) that is weaker in DCN experiments (Figure 1c) is at 2153.2 cm^{-1} with a ^{13}C counterpart only 3.7 cm^{-1} to the red. The small carbon isotopic shift and the drop in intensity in a partially deuterated sample suggest a Be−H stretching mode. Because no calculation of a cyclic product molecule converged with a potential minimum, the only possible products for this band are HBeCN and HBeNC. Table 5 gives the BP86 and CISD calculated frequencies for isotopic product molecules. For HBeCN, the Be−H stretch is calculated by the BP86 method to shift 14.7 cm^{-1} due to mixing with the C≡N stretch, but HBeNC is calculated to shift only 1.5 cm^{-1}, in much better agreement with experiment. Also, the calculated intensities for the Be−H stretches are 305 and 275 km mol^{-1} for $HBeN^{12}C$ and $HBeN^{13}C$ and 61 and 9 km mol^{-1} for $HBe^{12}CN$ and HBe^{13}-CN, further suggesting that the 2153.2/2149.5-cm^{-1} bands are due to the Be−H stretching absorptions of HBeNC. The calculations predict the corresponding DBeNC absorption at 1646.4 cm^{-1}. The observed 1631.3 cm^{-1} band agrees well with this calculation and tracks with the other Be−H absorptions on photolysis and annealing.

In Figure 1a, the BeNC peak at 2088.7 cm^{-1} has a shoulder band labeled C. The corresponding $BeN^{13}C$ absorption in Figure 1b has no such shoulder. Also, the intensity of this band is much reduced in Figure 1c, suggesting not only that this peak corresponds to a product distinct from BeNC, but also that this species contains hydrogen. Because frequencies in this region typically are due to C≡N stretches of isocyanide complexes, such as BeNC, this band must arise from HBeNC. According to Table 5, BP86 calculations predict this mode at 2066.9 cm^{-1}, in excellent agreement with experiment. For DBeNC, this calculated frequency shifts to the blue at 2078.4 cm^{-1}. For HBeNC, mixing between the Be−H and C≡N stretching modes forces the C≡N frequency to the red, but such mixing is absent in DBeNC. The peak in Figure 1c which best matches the calculation is at 2098.6 cm^{-1}, a band which tracks with the HBeNC absorption.

For $HBeN^{13}C$, there is no obvious C≡N stretching absorption, but one expects an isotopic shift similar to that for the other isocyanide product, BeNC. The BP86 calculations predict this frequency to be 2030.3 cm^{-1}. Because the other isotopic calculations are approximately 20 cm^{-1} too low, the C≡N stretch of $HBeN^{13}C$ should occur at about 2050 cm^{-1}, near the $BeN^{13}C$ peak, but no separate intense absorption can be observed in the spectrum. Upon photolysis, the A band of Figure 1b, which is noticeably larger than the A band of Figure 1a prior to photolysis, decreases in intensity, but to a lesser degree than for the ^{12}C experiments. A slight shift in the band profile can also be detected. Because the C bands increase in intensity and because the BP86 calculations predict the frequency of $HBeN^{13}C$ to be near this absorption, this A band must consist of two components: a strong BeNC absorption and a weaker HBeNC absorption. Given the resolution of the instrument, it is impossible to determine the exact frequency of $HBeN^{13}C$, but deconvolution of the spectra following photolysis gives a HBeNC frequency of 2050.9 cm^{-1} versus 2050.8 cm^{-1} for BeNC.

HBeNC has not only a C≡N stretch of nearly the same frequency as that of BeNC but also a Be−N stretch close in energy to that of BeNC. The C band in Figure 2a is much less intense in Figure 2c and tracks with the C bands of Figure 1. These peaks, then, are assigned to HBeNC. The BP86 calculations listed in Table 5 are in excellent agreement with experiment. For DBeNC, the band in Figure 2c at 895.6 cm^{-1} clearly tracks with the 912.4-cm^{-1} band of residual HBeNC. Although the calculations predict a larger deuterium isotopic shift, the experimental evidence indicates that deuteration shifts the Be−N stretching mode a relatively small amount. Because this isotopic shift is so small and the frequency shift of this mode from that of BeNC is also quite small, hydrogen does not appear to affect this vibrational mode of the isocyanide molecules.

The final observable mode for HBeNC is the doubly degenerate linear hydrogen bending mode predicted at 565.0 cm^{-1} for both ^{12}C and ^{13}C with a hydrogen isotopic shift of approximately 100 cm^{-1}. The doublet at 525.4 and 521.7 cm^{-1} among a cluster of peaks does not shift with carbon isotopic substitution and is assigned to this mode with the splitting possibly due to degeneracy breaking by the matrix environment. In Figure 3c, the stronger doublet at 422.1 and 418.0 cm^{-1} tracks with the HBeNC bands and exhibits a reasonable deuterium isotopic shift based on the calculations. Although the BP86 calculations are less accurate for these bending motions than for stretching vibrations, they are still nearly always within 10% of the experimental values.

Table 5 also reports CISD calculations with the 6-311G* basis set on HBeNC and HBeCN. Note that the isotopic ratios are similar to those of the BP86 method, but further displaced from the observed values. Although CISD calculations are more sophisticated than BP86 calculations and require much greater computation time, the BP86 calculations better enable identificaiton of products in these experiments.

Species D: HBeCN. The absorptions labeled D in Figure 1 also belong to a product with hydrogen. Although the frequencies of these peaks are consistent with both Be−H and C≡N stretches, the large carbon isotopic shift and relatively small hydrogen isotopic shift indicate that these are C≡N stretches. These frequencies are also more consistent with a cyanide product than with an isocyanide product. Calculations on

HBeCN (Table 5) give a C≡N stretching frequency approximately 20 cm^{-1} higher than the observed values for each of the isotopomers, in excellent agreement with experiment.

Calculated intensities of these absorptions are 167, 213, and 86 km mol^{-1} for $HBe^{12}CN$, $HBe^{13}CN$, and $DBe^{12}CN$, respectively, suggesting mixing with the nearby Be−H stretching mode. Because all of the bands labeled D track with each other and because the Be−H stretching frequency predictions are only 1% higher than the frequencies at 2128.6 and 2116.7 cm^{-1} for ^{12}C and ^{13}C, these absorptions must be due to the Be−H stretch of HBeCN. The calculated intensities for these peaks are 61 and 9 km mol^{-1} for ^{12}C and ^{13}C, suggesting preferential mode mixing for one of the isotopes. Since the $HBe^{13}CN$ bands are much closer in energy, the mode mixing must be greater in $HBe^{13}CN$ than in $HBe^{12}CN$. The C≡N stretching intensity of $HBe^{13}CN$ is greatest and the Be−H stretch intensity is lowest because mode mixing has transferred intensity from the latter to the former. Similarly for DBeCN, the C≡N stretch intensity is lowest because there is no mode mixing. The Be−D vibration, predicted at 1627.8 cm^{-1}, appears at 1642.1 cm^{-1}, with again approximately 1% difference between experiment and theory. For this peak, the lack of mode mixing makes it more intense than its HBeCN counterparts.

For the mixed C≡N and Be−H stretching modes in HBeCN, the carbon 12/13 ratios (observed, BP86, CISD) are (1.0172, 1.0163, 1.0214) and (1.0055, 1.0069, 1.0018), respectively. Clearly, the BP86 calculation more accurately reflects the observed mode mixing.

Like BeCN, HBeCN has a Be−C stretching vibration near 800 cm^{-1}. As with HBeNC and BeNC, this Be−C mode shifts a small amount upon addition of hydrogen to the beryllium atom. As shown in Table 5, calculations predict these frequencies extremely well. Unlike in HBeNC, the hydrogen isotopic shift in HBeCN is significant and agrees very well with the BP86 predictions. For the three stretching modes in HBeCN, the BP86 calculated frequencies deviate no more than 1.2% from experiment for any isotopic combination.

The linear bending mode for HBeCN is predicted to appear near that of HBeNC, but with a small carbon isotopic shift. With carbon three atoms away from the hydrogen, as in HBeNC, isotopic substitution does not noticeably affect the frequency, but with carbon only two atoms away, as in HBeCN, a small shift should be observed. On the blue shoulder of the cluster of peaks comprising the HBeNC bands, a peak shifts from 530.1 to 528.3 cm^{-1} upon ^{13}C substitution. The presence of a second doublet other than one due to HBeNC in the DCN experiments, which tracks with the bands labeled D, indicates that this second linear bend is due to HBeCN. As with HBeNC, the calculations do not predict these frequencies as well as for the stretching modes, but are still quite good nonetheless. Because the degeneracy of this linear H bend is broken in DBeCN, it is likely that the degeneracy is also broken for HBeCN, but the HBeNC bands prevent the observation of the other member of this doublet to the red of the observed peak.

Reaction Mechanisms. Given the relative simplicity of the Be/HCN system and the lack of observed dicyanide complexes, the major pathway to product formation is via insertion:

$$Be^* + HCN \rightarrow [HBeCN]^\dagger$$

The growth of some products on photolysis and the general decrease of product absorptions on annealing suggest that energetic Be atoms are required for the insertion reaction. Recent studies have provided convincing evidence that ^3P Be atoms from the ablation process are the reactive species in these experiments.[7−12] The excited HBeCN molecule can either relax and be trapped in the argon matrix or form other products. For example, BeCN can form via H atom elimination, HBeNC via rearrangement, and BeNC via rearrangement and H atom elimination.

The most intense absorptions in the spectra of the Be + HCN reaction products correspond to the radical BeNC. Although the calculated intensity of this absorption is also the strongest among all the products observed, this band is too intense for BeNC to be anything other than a major product, if not the most abundant new product. The insertion mechanism probably yields more BeCN than BeNC because of a more direct path to product formation, but far more BeNC is observed. This suggests a possible alternate mechanism similar to a S_N2 reaction:

$$Be^* + NCH \rightarrow [BeNC]^\dagger + H \rightarrow BeNC + H$$

Another possibility is Be bonding to a CN fragment formed from the radiation in the ablation process, but the "S_N2" mechanism would yield preferentially more BeNC compared to BeCN. Such disproportionation in the formation of BeNC might explain why these peaks are reduced so drastically on photolysis while those of BeCN increase tremendously—the photolysis initiates an equilibration process between the two products to bring their relative concentrations closer. The ultraviolet radiation apparently has sufficient energy to overcome the barrier to interconversion:

$$BeNC \overset{UV}{\rightleftharpoons} BeCN$$

The high yield of HBeNC relative to HBeCN may result from rapid rearrangement of the insertion product to the more stable isomer, but another "S_N2" reaction may be the reason for the relatively high yield. First, Be abstracts an H atom to form BeH, which is also observed in the product spectrum, then the following reaction can take place:

$$[HBe]^\dagger + NCH \rightarrow [HBeNC]^\dagger + H \rightarrow HBeNC + H$$

Comparison of Frequency Calculations. The apparent superiority of the BP86 functional over more sophisticated methods can be explained by recognizing that all of these methods calculate harmonic vibrational frequencies. Anharmonicity in the products lowers the experimental vibrational frequencies and is the reason the B3LYP, MP2, and CISD methods generally overestimate the observed frequencies. In a comparison of various Hartree−Fock and DFT methods, Scott and Radom showed that the BP86 calculations tend to overestimate bond lengths, thereby underestimating harmonic stretching frequencies.[36] This shortcoming of the BP86 method actually enables these calculations to predict vibrational frequencies of the beryllium−hydrogen cyanide products with excellent precision. That this result is fortuitous should be noted.

Nevertheless, HBeNC and especially HBeCN required more precise calculations than usual because of mixing between the Be−H and C≡N stretching modes. Whereas the BP86 calculations with 6-311G* basis sets were accurate in predicting the isotopic shifts observed in the experiments, the other methods did not fare as well because of this mode mixing. With use of the BP86 functional with the cc-pVDZ plus D95* basis sets, the predicted carbon-13 shifts of the Be−H and C≡N stretches in HBeCN are 20.3 and 30.2 cm^{-1}, which is somewhat less accurate than the values determined with the 6-311G* basis sets. As Table 3 shows, the difference when using different basis

(36) Scott, A. P.; Radom, L. *J. Phys. Chem.* **1996**, *100*, 16502.

sets is relatively small for BeCN and BeNC, and the same can be said for HBeCN and HBeNC. With the B3LYP method, however, the differences are more pronounced, with carbon-13 shifts of 7.6 and 44.5 cm^{-1} predicted by this method. Although the B3LYP, MP2, and CISD methods are probably superior to the BP86 method for calculating geometries and harmonic frequencies, the BP86 functional provides clear advantages for identifying new reaction products from their experimental (i.e., anharmonic) frequencies.

Conclusions

The major products of the reaction of laser ablated beryllium atoms with hydrogen cyanide are BeNC, BeCN, HBeNC, and HBeCN. No products with a Be(CN) ring are observed. Because of the low concentration of HCN in the Ar mixture, no products with two or more CN groups were detected. The C≡N and Be−N stretching frequencies are similar for both BeNC and HBeNC, indicating that the presence of the hydrogen atom has little effect on these modes. The same is true for the Be−C stretches of HBeCN and BeCN, but not for the C≡N stretch. In HBeCN, mixing between the nearly isoenergetic Be−H and C≡N stretching modes tends to push the C≡N vibrational frequencies higher and the Be−H frequencies lower. The effect is most pronounced for $HBe^{13}CN$, leading to an unusually large 11.8 cm^{-1} carbon isotopic shift for the Be−H stretch and a loss of intensity in this mode relative to that of $HBe^{12}CN$.

For the products observed in these experiments, BP86 calculations have provided an excellent guide to identification of the product bands. For most of the absorptions, these calculations predict vibrational frequencies within 1% of the experimental values. Despite complexities in the spectra, such as mode mixing in HBeCN and the coincidence of absorptions in $BeN^{13}C$ and $HBeN^{13}C$, the BP86 calculations with 6-311G* basis sets have enabled the identification of all four major products with confidence. Of particular importance is the comparison of isotopic frequency shifts (or ratios) as a description of normal modes[37] to determine the degree of agreement between theory and experiment. The BP86 calculations with a more inclusive basis set, cc-pVDZ plus D95*, and the more sophisticated B3LYP and MP2 calculations are inferior at predicting the product vibrational frequencies. Although all methods predict harmonic frequencies, the BP86 calculations tend to overestimate bond lengths in the geometry optimization, leading to lower energy predictions for stretching vibrations. These predictions are, therefore, closer in energy to the observed (i.e., anharmonic) values. The CISD method succeeds at predicting vibrational frequencies nearly as well as the BP86 method, but the increase in computation time makes using this method impractical for the purposes of this study.

The density functional calculations show that the BeNC, BeCN, HBeNC, and HBeCN molecules are linear. These compounds further illustrate the role of beryllium bonding in small linear molecules and complement earlier studies with HBeH (the textbook example of sp hybridization), HBeCCH, BeCCH, and HBeOBeH.[7,11,12]

Acknowledgment. This work was supported by the Air Force Office of Scientific Research. Calculations were performed on the University of Virginia SP2 machine. $K^{13}CN$ was kindly donated by Cambridge Isotope Laboratories.

JA970740G

(37) Martin, J. M. L.; Taylor, P. R.; Hassanzadeh, P.; Andrews, L. *J. Am. Chem. Soc.* **1993**, *115*, 2510.